Journal of ELECTRONIC MATERIALS, Vol. 44, No. 6, 2015
DOI: 10.1007/s11664-014-3562-y

Analysis of Thermal Losses for a Variety of Single-Junction Photovoltaic Cells: An Interesting Means of Thermoelectric Heat Recovery

BRUNO LORENZI,[1,2] MAURIZIO ACCIARRI,[1,3] and DARIO NARDUCCI[1,4]

1.—Department of Materials Science, University of Milano Bicocca, Milano, Italy. 2.—e-mail: b.lorenzi2@campus.unimib.it. 3.—e-mail: maurizio.acciarri@unimib.it. 4.—e-mail: dario.narducci@unimib.it

Exploitation of solar energy conversion has become a fundamental aspect of satisfying a growing demand for energy. Thus, improvement of the efficiency of conversion in photovoltaic (PV) devices is highly desirable to further promote this source. Because it is well known that the most relevant efficiency constraint, especially for single-junction solar cells, is unused heat within the device, hybrid thermo-photovoltaic systems seem promising . Among several hybrid solutions proposed in the literature, coupling of thermoelectric and PV devices seems one of the most interesting. Taking full advantage of this technology requires proper definition and analysis of the thermal losses occurring in PV cells. In this communication we propose a novel analysis of such losses, decoupling source-dependent and absorber-dependent losses. This analysis enables an evaluation of the actual recoverable amount of energy, depending on the absorber used in the PV cell. It shows that for incoming solar irradiation of 1000 W/m^2, and depending on the choice of material, the maximum available thermal power ranges from 380 W/m^2 (for single-crystal silicon) to 130 W/m^2 (for amorphous silicon).

Key words: Thermoelectric, photovoltaic, thermal losses

INTRODUCTION

From analysis of the energy fluxes within a single-junction photovoltaic (PV) device it is easy to understand that the largest factor limiting efficiency is unavoidable decoupling between the energy source (the Sun) and the absorbing material. Whereas the solar spectrum is continuous over a wide range of frequencies, the device is capable of efficient conversion solely for photons at the frequency corresponding to the energy gap (E_g) of its absorbing material. The other part of the spectrum is either not completely absorbed ($E < E_g$) or is absorbed but only partially converted into heat ($E > E_g$). Such energy losses (with other optical and electrical losses) constrain the PV efficiency (η_{PV}) to below the Shockley–Queisser limit;[1] values are approximately 30%, depending on the absorber E_g.[2] A possible means of overcoming this limit is implementation of multi-junction solar cells in which more materials operate as absorbers. On this premise, many different devices have been proposed in literature (so-called "third-generation PV"). These include tandem cells, three and four-junction solar cells, up–down conversion devices, and light concentrators. More recently, an alternative approach has become popular. Energy wasted by the single-junction PV device is converted into useful work by heat recovery.[3–7] We will refer to this class of devices as "hybrid thermo–photovoltaic systems" (HTPVs). The method used to convert heat into useful work may differ, and an explicit account of the dependence of recoverable power on the absorber material used in the PV cell has not yet been given for any of the devices.

In this paper we focus on a special sub-class of HTPV device in which a PV cell is coupled, both thermally and electrically, in series with a thermoelectric

(Received July 15, 2014; accepted November 27, 2014;

generator (TEG). We will refer to these as "hybrid thermo-electric-photovoltaic devices" (HTEPVs). After analysis of the loss processes involved in a single-junction solar cell, we show how the absorber characteristics are crucial to the amount of power that can be recovered by the TEG. We will also show how this analysis should also determine the choice of the TEG characteristics to achieve lossless hybridization, and thus to maximize the overall output power.

LOSSES IN SINGLE-JUNCTION PV

It is clearly apparent that increasing the efficiency of conversion by single-junction solar cells requires proper definition and identification of all sources of loss. The efficiency of a generic PV system is simply the ratio of output power to input power, i.e.:

$$\eta_{PV} \equiv \frac{P_{out}}{P_{in}} = \frac{V_{oc} I_{sc} FF}{\Phi_{Sun} S_{cell}} \tag{1}$$

where V_{oc}, I_{sc}, and FF are, respectively, the open-circuit voltage, the short-circuit current, and the filling factor, and Φ_{Sun} and S_{cell} are the solar radiation intensity and the device area. Thermodynamically, the maximum efficiency η_C achievable by a solar cell is equal to the Carnot efficiency, i.e. $\eta_C = 1 - T_{cell}/T_{Sun}$, where T_{cell} is the device (cold side) temperature and T_{Sun} is the Sun temperature. According to Landsberg[8] this formula should be modified taking into account the non-zero radiation emitted by the absorber:

$$\eta_{max} \equiv \frac{P_{max}}{P_{in}} = 1 - \frac{3}{4}\left(\frac{T_{cell}}{T_{Sun}}\right) + \frac{1}{3}\left(\frac{T_{cell}}{T_{Sun}}\right)^4 \tag{2}$$

Taking $T_{cell} = 300$ K and $T_{Sun} = 6000$ K one obtains an efficiency of 93.33%.

However, Shockley and Queisser[1] showed how, in a single-junction device, the actual achievable efficiency is bound to much lower, because of several types of energy loss. It may be useful to group these as follows:

1. **Optical Losses** (L_1):
   (a) contact grid shadow (L_{1a})
   (b) radiation reflection (L_{1b})
   (c) spurious absorption (L_{1c})
2. **Source-absorber decoupling losses** (L_2):
   (a) non-absorbed photons with $E < E_g$
   (b) thermalization of hot carriers (photons with $E > E_g$)
   (c) efficiency degradation because of cell heating
3. **Thermal losses** (L_3), namely the Joule effect
4. **Electrical and recombination losses** (L_4):
   (a) non-unitary quantum efficiency
   (b) $qV_{oc} < E_g$

Because such losses occur sequentially, the actual output power P is:

$$P = P_{max} \prod_{n=1}^{4} L_n \tag{3}$$

Thus the efficiency η is:

$$\eta = \frac{P}{P_{in}} = \eta_{max} \prod_{n=1}^{4} L_n \tag{4}$$

As mentioned, the largest contribution to the overall loss comes from the L_2 term. As will be shown in the sections below, L_2 corresponds to $\approx$ 60% of the overall incoming power, the other three terms total less than 20%. One may also note that the first two contributions to L_2 are independent processes. Instead, cell heating is a direct consequence of thermalization of the absorbed photons. Thus one may rewrite L_2 as:

$$L_2 = L_{2a} + L_{2b} + L_{2b}\chi \tag{5}$$

with $0 \leq \chi \leq 1$.

ESTIMATION OF SOURCE-ABSORBER DECOUPLING LOSSES

Loss as a Result of Non-Absorbed Photons

The first contribution to L_2 comes from what is often called the thermal portion of the solar spectrum.[6] L_{2a} is a function of E_g, increasing with it. Let $\Phi_{Sun}(E)$ be the solar spectral irradiance, defined over $[E_m, E_M]$ (Fig. 1a). Thus:

$$L_{2a}(E_g) = \frac{\int_{E_m}^{E_g} \Phi_{Sun}(E)dE}{\int_{E_m}^{E_M} \Phi_{Sun}(E)dE} \tag{6}$$

Computing $\Phi_{Sun}(E)$ using standard values of the terrestrial solar irradiance (A.M. 1.5)[9] one finds that, as expected, L_{2a} increases almost linearly with E_g, ranging from ~16% for bulk silicon to more than 50% for thin-film technology (Fig. 1b).

Thermalization of Hot Carriers

Following the same approach as used for L_{2a} one obtains:

$$L_{2b}(E_g) = \frac{\int_{E_g}^{E_M} n_\gamma(E)(E - E_g)dE}{\int_{E_m}^{E_M} n_\gamma(E)(E - E_g)dE} \tag{7}$$

where n_γ is the number of incoming photons with energy between E and $E + dE$ and $(E - E_g)$ is the amount of energy released by every carrier upon thermalization. Because $n_\gamma(E)$ is proportional to the incoming spectral power, one may replace it with $\Phi_{Sun}(E)$ in Eq. 7. Figure 1b displays L_{2b} as a function of the absorber material energy gap. For silicon,

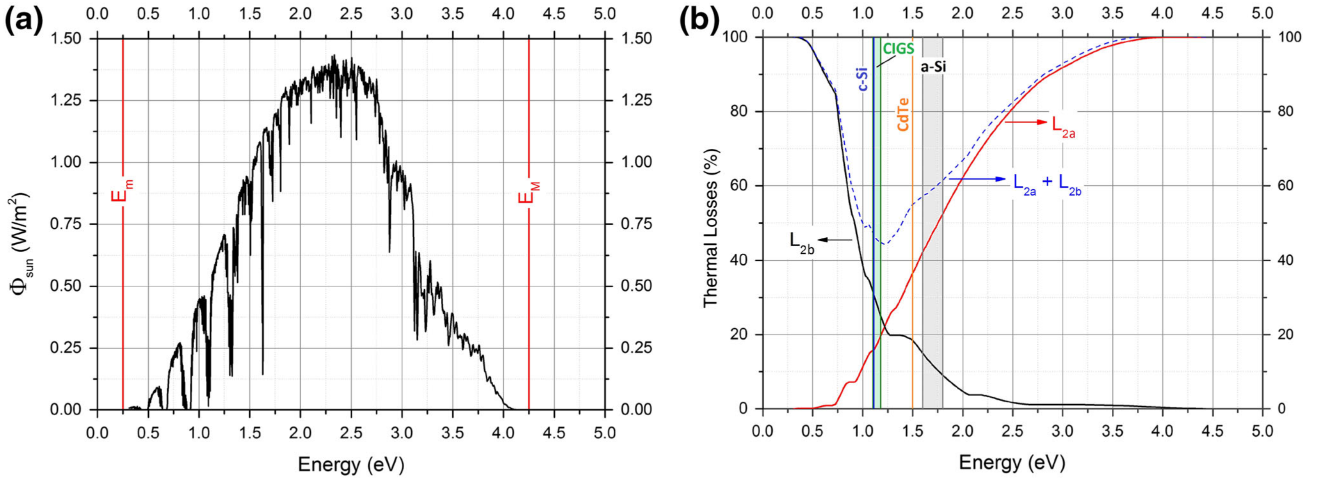

Fig. 1. (a) Plot of $\Phi_{\mathrm{Sun}}(E)$ in the case of A.M. 1.5 solar spectrum. (b) Evaluation of L_{2a} and L_{2b} as a function of E_g. The E_g values of the absorber materials considered in this paper are highlighted.

$L_{2b} \approx 30\%$ whereas smaller values (down to 10%) are obtained for materials with larger E_g. Note that $L_{2b}(E)$ has a larger slope than $L_{2a}(E)$.

Degradation as a Result of Cell Heating

The third term of L_2 depends on the cell temperature and directly depends on the second decoupling loss. It is actually well known that an inverse correlation exists between PV efficiency and cell temperature. Following Luque and Hegedus[2] the L_{2c} term may be modeled as a function of the intrinsic carrier concentration and of its dependence on the temperature. An increase of the carrier concentration with T leads to a larger dark saturation recombination current, affecting, in turn, the open-circuit voltage V_{oc}. Because the short-circuit current is marginally affected by the increase of the temperature, approximately linear dependence of efficiency on the cell temperature is observed. Thus, under standard test condition (STC; i.e. solar radiation flux of 1000 W m^{-2}, A.M. 1.5, temperature of 25°C):

$$\eta = \eta_{STC} - (T_{cell} - 25^{\circ}\mathrm{C})\gamma_{rel} = \eta_{STC} - L_{2c} \qquad (8)$$

which immediately leads to L_{2c}. Temperature coefficients γ_{rel} for every material considered in this paper can be found in the literature.[10]

Several methods have been proposed for proper determination of T_{cell}.[11] The most common approach assumes an energy flux balance between incoming and outgoing power in the PV system, leading to:

$$\tau\alpha\Phi_{Sun} = U_L(T_{cell} - T_a) \qquad (9)$$

where τ and α are, respectively, the glazing transmittance and the PV layer absorbance, T_a is the ambient temperature, and U_L is the thermal loss coefficient, which has the dimensions of a thermal conductance. Considering the cell-heating process as the sole consequence of thermalization of the hot photogenerated carriers, Eq. 9 becomes:

$$L_{2b}\Phi_{Sun} = U_L(T_{cell} - T_a) \qquad (10)$$

so

$$L_{2c} = L_{2b}\Phi_{Sun}\frac{\gamma_{rel}}{U_L} \qquad (11)$$

which, as expected, is proportional to L_{2b}.

The only unknown term in Eq. 11 is U_L. A PV device exchanges energy with the environment radiatively and convectively (at least) from both the top and bottom of the module.[12] As a result, wind speed, the type of mounting, the materials used in the top and bottom finalizing layers, and the way the cell is encapsulated determine U_L. A range of U_L values for different types of PV configuration can be found in the literature.[11,13]

Figure 2a shows the dependency of T_{cell} on absorber energy gap for different values of U_L. For any given value of U_L, T_{cell} increases with decreasing values of E_g , because of its proportionality to L_{2b}. This dependency is highly relevant for small U_L and becomes negligible for large U_L because of the heat flux between the cell and the environment. A likely trend is shown in Fig. 2b, which shows the dependence of L_{2c} on U_L for a given absorber.

HYBRID THERMOELECTRIC–PHOTOVOLTAIC SYSTEMS

In this section we discuss HTPV devices in which a TEG is coupled with a PV cell. The basic idea is to connect a TEG both electrically and thermally downstream of the PV cell (Fig. 3). The TEG will then convert the thermal flux flowing between the PV cell and the environment. Park et al.[7] recently

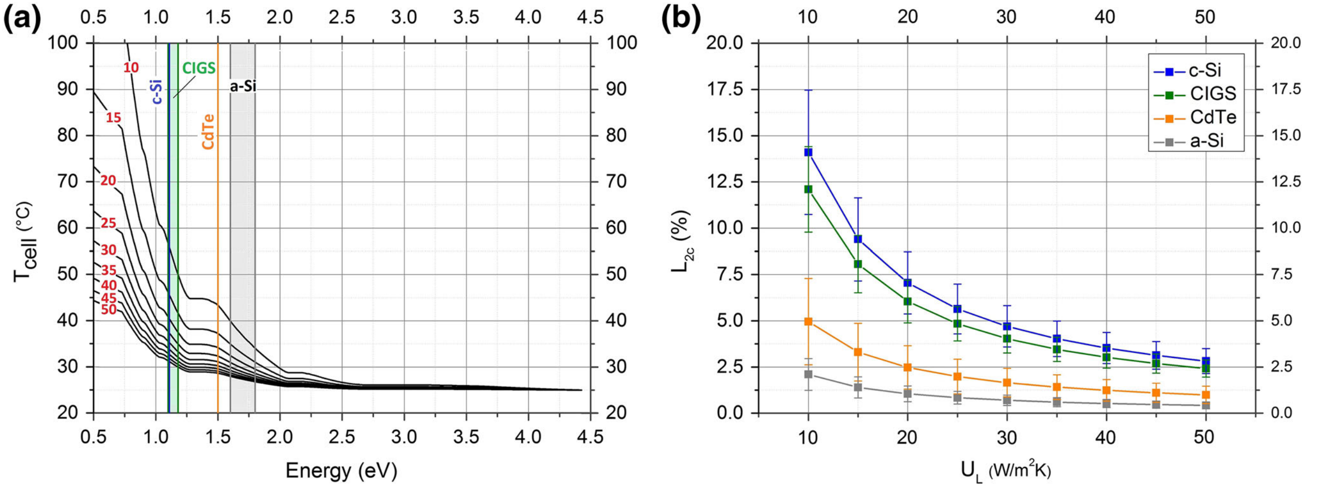

Fig. 2. (a) Plot of T_{cell} as a function of the absorbing material E_g for different values of U_L between 10 and 50 W m^{-2}K^{-1}. (b) Values of L_{2c} as a function of U_L for four types of absorbing material. Bars indicate the range of values as a result of the variability of U_L.

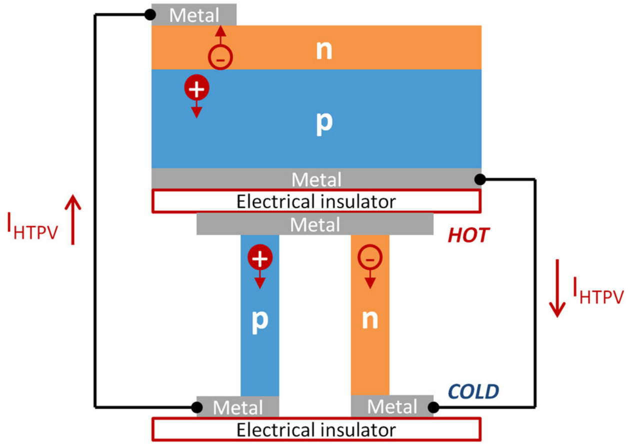

Fig. 3. Schematic diagram of the HTEPV device, in which a TEG device is connected thermally and electrically in series with the PV cell. For simplicity we have drawn a TEG composed of just a thermocouple.

showed how lossless hybridization is necessary to achieve an increase in overall power output. Their hybridization approach takes into account the relationship between three variables, the TEG internal electrical resistance R_{el}, the TEG operating voltage V_{TEG}, and the current flowing within the hybrid device I_{HTEPV}.

We will show below how the PV absorber characteristics and the efficiency losses of the PV part must also be considered to maximize the performance of the hybrid device. Whereas for a given TEG the electrical resistance R_{el} is fixed, both I_{HTEPV} and V_{TEG} strongly depend on PV performance. The TEG thermovoltage is given by:

$$V_{TEG} = N(\alpha_p - \alpha_n)\Delta T \tag{12}$$

where N is the number of TEG pairs, α_p and α_n are the Seebeck coefficients of the p and n legs, and ΔT is the temperature difference between the hot and cold side of the TEG. ΔT is, in turn, a function of the incoming power and of the TEG internal thermal resistance (R_{th}), i.e.:

$$\Delta T = T_{cell} - T_a = qR_{th}S_{TEG} \tag{13}$$

where $q = (L_{2b} + L_{2b})\phi_{Sun}$ is the heat flow from the PV cell and S_{TEG} is the TEG area. Similar considerations apply to I_{HTEPV}. Because[7]:

$$I_{HTEPV} = I_{sc} - I_0 \exp\left(\frac{eV_h}{k_B T}\right) - \frac{V_h}{R_{sh}} \tag{14}$$

and

$$V_h = V - V_{TEG} + I_{HTEPV}(R_s + R_{TEG}) \tag{15}$$

(where I_0, R_{sh}, and R_s are the dark saturation current, the cell shunt resistance, and the cell series resistance, respectively), I_{HTEPV} is found to depend through V_h on V_{TEG}. Hence, the current flowing throughout the HTEPV cell clearly depends on the characteristics of the absorber. In contrast, R_{th} affects the heat flow between the PV cell and the environment, and thus the overall thermal loss coefficient:

$$U_L = U_L^{PV} + \frac{1}{R_{th}} \tag{16}$$

where U_L^{PV} is the contribution to the thermal loss coefficient as a result of the PV part only. Thus R_{th} controls L_{2c} through U_L. As a result, optimum choice of TEG properties maximizing the efficiency of the hybrid device depends both on the characteristics of the PV absorber and on the TEG thermal resistance. Figure 4 shows the L_2 components for some common absorbing materials. Bars for the L_{2a} component reflect the E_g variability of the corresponding material, and L_{2b} and L_{2c} bars depend on U_L, typically ranging between 15 and 30 W/m^{2}K for non-cooled PV cells.[11,13] One may easily verify that

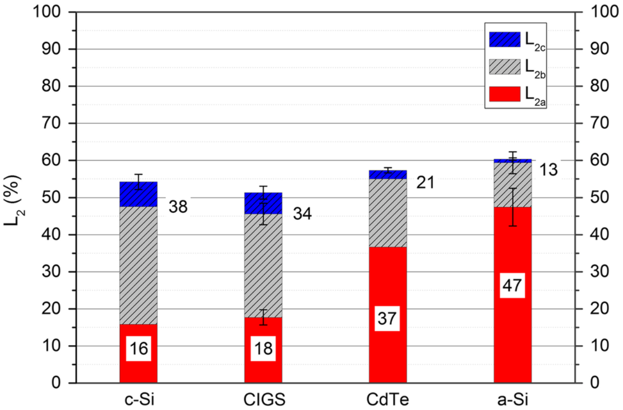

Fig. 4. Histograms showing the contribution of L_2 for different technology. The numbers on the bars are L_{2a} and $L_{2b} + L_{2c}$ values. Error bars show the range of minimum and maximum values for each L_2 component. Bars on L_{2a} result from the variability of the energy gaps of CIGS and a-Si. Bars on L_{2b} and L_{2c} are, instead, because of the variability of U_L.

although the total value of L_2 is nearly the same for all materials, ranging between 55% and 65%, the contribution of L_{2a} increases moving from c-Si to a-Si. Instead, $(L_{2b} + L_{2c})$ shows exactly the opposite trend.

In an HTEPV device such as that shown in Fig. 3 the TEG may only recover the $L_{2b} + L_{2c}$ fraction of the lost input power, because the L_{2a} fraction (totally non absorbed) has no thermal effects. Thus it is straightforward to conclude that, in the important case of c-Si, the maximum recoverable power is $(L_{2b} + L_{2c})\Phi_{Sun} = 380\ \mathrm{W/m^2}$ (i.e. 38% of Φ_{Sun}). This amount decreases as the energy gap of the absorber is increased, becoming 130 W/m^2 (13% of Φ_{Sun}) for amorphous silicon.

It may be worth stressing that the actual values of L_{2b} and L_{2c} depend on U_L—and thus on R_{th}. The maximum HTEPV output power is:

$$P_{HTEPV}^{max} = P_{PV}^{max} + P_{TEG}^{max} \tag{17}$$

Because η decreases with temperature (Eq. 8), the maximum efficiency for non-cooled cells is η_{STC}. Thus, P_{PV}^{max} follows from Eqs. 10 and 11, i.e.:

$$P_{PV}^{max} = P_{STC}(1 - L_{2b}\chi_h) \tag{18}$$

where $P_{STC} = \eta_{STC} P_{in}$ is the cell power output at the STC temperature and a dimensionless coefficient $\chi_h \equiv \frac{\Phi_{Sun}\gamma_{rel}}{U_L} = \Phi_{Sun}\gamma_{rel}\left(\frac{1}{U_L^{PV}} + R_{th}\right)$ is introduced. For the thermoelectric component, by use of Eqs. 12 and 13, one obtains, instead:

$$P_{TEG}^{max} = \frac{1}{4}\frac{\left[N(\alpha_p - \alpha_n)\Phi_{Sun} L_{2b} R_{th} S_{TEG}(1 + \chi_h)\right]^2}{R_{el}} \tag{19}$$

Optimization of P_{HTEPV}^{max} is not trivial, because of the interdependence of the properties of the material, and is beyond the scope of this paper.

SUMMARY AND CONCLUSION

We report a novel scheme for evaluation of the recoverable thermal losses of single-junction solar cells, which emphasizes the importance of the characteristics of the PV absorber, especially its energy gap, to the total loss. In previous publications, hybrid thermoelectric–photovoltaic devices were reported to enable enhancement of the overall output power if the HTEPV device properties were appropriately balanced. We have shown that the amount of power recoverable from hybrid configurations is strictly dependent on cell absorber material. Consequently, the maximum TEG output power is also determined by the optical characteristics of the absorber. Thus proper optimization of the HTEPV device must take into account the absorber properties, which should, in turn, guide selection of the properties of the hybrid device.

ACKNOWLEDGMENTS

This work was supported by FP7-NMP-2013-SMALL-7, SiNERGY (Silicon Friendly Materials and Device Solutions for Microenergy Applications) Project, Contract n. 604169.

REFERENCES

1. W. Shockley and H. Queisser, *J. Appl. Phys.* **32**, 510 (1961).
2. A. Luque and S. Hegedus, *Handbook of Photovoltaic Science and Engineering* (Wiley, Chichester, 2002), p. 99.
3. D. Kraemer, L. Hu, A. Muto, X. Chen, G. Chen, and M. Chiesa, *Appl. Phys. Lett.* **92**, 243503 (2008).
4. T.T. Chow, *Appl. Energy* **87**, 365 (2010).
5. B. Parida, S. Iniyan, and R. Goic, *Renew. Sust. En. Rev.* **15**, 1625 (2011).
6. N. Wang, L. Han, H. He, N. Parkb, and K. Koumoto, *En. Env. Sci.* **4**, 3676 (2011).
7. K. Park, S. Shin, A.S. Tazebay, H. Um, J. Jung, S. Jee, M. Oh, S. Park, B. Yoo, C. Yu, and J. Lee, *Sci. Rep.* **3**, 2123 (2013).
8. P. Landsberg and G. Tonge, *J. Appl. Phys.* **51**, R1–20 (1980).
9. ASTM G173, (ASTM International, West Conshohocken, PA, 2012) http://www.astm.org/Standards/G173.htm.
10. A. Virtuani, D. Pavanello, and G. Friesen, Proceedings 25th UE PVSEC, Spain 4248 (2010).
11. E. Skoplaki and J.A. Palyvos, *Ren. En.* **34**, 23 (2009).
12. M.K. Fuentes, *Sandia Rep. 85–0330* (Sandia National Laboratory, Albuquerque, 1987).
13. T. Nordmann and L. Clavadetscher, Proceedings 3rd WCPE, Japan 2243 (2003).